# Solidification and metastable phase formation in conventional and planar flow cast Ti-48.8at%Al-2.2at%V

G. Shao, T. Grosdidier, P. Tsakiropoulos

JOURNAL DE PHYSIQUE IV
Colloque C7, supplément au Journal de Physique III, Volume 3, novembre 1993 

# Solidification and metastable phase formation in conventional and planar flow cast Ti-48.8at%Al-2.2at%V

G. SHAO, T. GROSDIDIER and P. TSAKIROPOULOS

*Department of Material Science and Engineering, University of Surrey, Guildford GU2 5XH, U.K.*

**Abstract** : The solidification paths and subsequent solid state transformations of conventional and planar flow cast Ti-48.8at.%Al-2.2at.%V alloy were studied. At low cooling rates, $\alpha$ is the first phase to form from the melt. The primary hexagonal dendrites subsequently underwent the $\alpha \rightarrow \alpha_2 + \gamma$ solid state transformation resulting in a lath structure made of {111} $\gamma$ twins separated by thin $\alpha_2$ layers. The Al rich interdendritic areas consisted of $\gamma$ solidified from the segregated melt. Under higher cooling rates, $\gamma$ is the first phase to form from the melt. This was confirmed by the lath-free microstructure of the dendrites and by the fact that these dendrites were richer in Al than the interdendritic area leading to reverse segregation. The Al lean areas were $\gamma$ formed from an $\alpha$ parent phase by either the massive $\alpha \rightarrow \gamma$ or the $\alpha \rightarrow \alpha_2 + \gamma$ solid state transformations. For the largest melt undercoolings, the microstructure was free of chemical segregation and disordered $\gamma$ formed directly from the melt. Extremely fine networks of ordered domains were also observed, showing the subsequent ordering process of the $\gamma$ phase.

## I. Introduction

For aerospace applications there is at present a great deal of interest in TiAl base alloys with addition of vanadium, which has been reported to result in plasticity enhancement (1). This study examines the solidification paths and subsequent solid state transformations in a conventional and rapidly solidified Ti-48.8at.%Al-2.2at.%V alloy.

## II. Experimental procedure

The Ti-48.8at.%Al-2.2at.%V alloy was arc melted in a cold hearth and planar flow cast on a water cooled copper wheel. After processing, an analysis by IMI Titanium - Birmingham of the various cast materials gave values always below : Hydrogen : 15 wppm, Oxygen : 600 wppm, Nitrogen : 15 wppm. The microstructural characterizations were carried out on a JEOL 2000-fx transmission electron microscope, a PHILIPS EM400T with a LINK AN10000 EDX system, a CAMBRIDGE S250 electron scanning microscope and a JEOL JXA8600 EPMA system. TEM thin foils were prepared by ion beam thinning.

## III. Results

In the ingots conventionally cast at relatively low cooling rates $\alpha$ was the first phase to form from the melt and $\gamma$ formed in the interdendritic areas from the segregated melt. The segregated melt was richer in Al and leaner in Ti and V than the dendrites (Table 1). The microstructure of the dendrites was made of {111} $\gamma$ twins with $\alpha_2$ at some interfaces.

Rapid solidification processing was used to cast materials in the shape of ribbons or flakes with thicknesses in the range 20 to 800 μm. SEM observations of transverse sections and of the top surface morphology of these materials, together with chemical analysis and TEM characterization were undertaken to investigate the influence on the microstructure and solidification paths of the different thermal histories experienced through the ribbon thickness.

### III. 1. Transverse sections of the solidified materials.

In figures 1a and 1b are shown two typical backscattered scanning electron micrographs of transverse sections. In the thickest materials (over about 250/300 μm in thickness), a three zone solidification morphology was observed. The relative size of these different zones varied from one specimen to another or along the same solidified material. These variations are believed to be related mainly to differences in the local cooling conditions associated with the quality of the wheel/melt contact and the ribbon or flake thickness. Zone A is a low contrast layer of material observed at the wheel side of the ribbons. Its thickness varies from a few μm to up to about 50 μm. The microstructure consists of nearly equiaxed grains. Zone B is a columnar structure that grows from region A and is the main feature through the thickness in 150/300 μm thick material. Zone C is observed in the upper regions of the thickest flakes (over 300 μm in thickness). It exhibits a dendritic microstructure indicating slower cooling rates at the free side of the flakes. Figure 1c shows a SEM micrograph of the fracture surface of a thick flake that shows the dendritic structure at the surface. Some porosity was also present mainly at the upper region of the materials (figure 1a and 1b).

### III. 2. Top surface morphology of the solidified materials.

In figure 2 are shown SEM micrographs illustrating the different features observed on the top surface of cast materials of different thicknesses. As shown in figure 2a, the top surface for the thickest flakes (>350 μm) consisted of large dendrites with arms at 60° with respect to one another. This shows that the primary solidification phase was the hexagonal $\alpha$ phase. The interdendritic areas were made of smaller equiaxed grains formed from the segregated melt. The top surface of the 250/300 μm thick flakes showed the same trend (figure 2b) but the size of the hexagonal dendrites was smaller and the amount of segregate was reduced dramatically. For the thinner materials (50 μm and 100 μm in figure 2d and 2c respectively), the dendritic structure was not present and the top surface consisted of smaller features. In figure 2d the grains have the same appearance as those observed between the large hexagonal dendrites in figure 2a.

### III.3. Fine scale features and chemical segregation.

TEM investigations and chemical composition measurements were carried out in order to study some microstructural features of the different solidified zones described in section III.1. TEM observation and EDX analysis were carried out on thin foils sampled half way along the thickness of the 150 μm thick flakes (zone B) or at the wheel side of the 20 μm thick ribbons (zone A). The free side of the thickest flakes (zone C) was investigated by EPMA.

Free side of 400μm thick flakes.

The characteristic microstructure of the free-side of the 400 μm thick flakes is shown in figure 2a. As in conventionally cast material, EDX measurements showed that the interdendritic regions were leaner in Ti and richer in Al than the hexagonal dendrites (Table 1).

Middle section of 100/200 μm thick flakes.

The characteristic microstructure of the mid-section of the 100/200 μm consists of clear grains or/and dendrites surrounded by hazy interdendritic regions. An example of this microstructure is shown in figure 3. Diffraction experiments showed that the prevailing phase in both the dendrites and the interdendritic regions is γ. However, EDX measurements in the TEM showed that the segregated γ phase was always richer in Ti (and leaner in Al) than the adjacent γ dendrites (Table 1). The segregation was therefore reversed compared to the segregation observed at the free side of the ribbons where α was formed as the primary phase in solidification. The γ grains/dendrites were also virtually lath free. This confirms that the γ phase in these grains was not the result of a solid state transformation but formed directly from the melt. Other observations of the mid-section in 30μm ribbons (2) led to the same conclusion concerning the formation of the γ phase from the melt. The interdendritic areas consisted of γ laths associated with solid state transformation. TEM investigations of these laths showed two kinds of structure. The prevailing structure contained a high density of parallel γ laths oriented at 90° to one another around <100> (2). This structure was free of any $\alpha_2$ phase. The second structure consisted of {111} twin related γ laths with very thin layers of $\alpha_2$ present at some twins boundaries.

Wheel side of 20 μm thick ribbons.

At the wheel side of the 20 μm thick ribbons, no noticeable chemical segregation was found by EDX analysis in the TEM and γ was the only phase present. The microstructure was however quite complex and varied extensively from one region to another. Three different features were observed (a) ordered γ grains, (b) disordered γ grains and (c) grains containing fine networks of ordered domains. The fully ordered $L1_0$ γ grains were very similar to those observed by Hall and Huang (3) at the wheel side of binary Ti-48at%Al melt spun ribbons. The mechanism for the formation of this microstructure will be discussed elsewhere. The grains of disordered γ phase were microtwinned (2, 4). Finally, the microstructure observed within some other grains at the wheel side of the 20μm ribbons consisted of a very fine network of ordered domains corresponding to all possible different variants of the γ-TiAl phase (2, 4). These ordered domains are evidence of the beginning of a solid state ordering process within the disordered grains.

## IV. Discussion

Three different zones (equiaxed, columnar and dendritic) representing transitions in the solidification process have been observed through the thickness of the thickest rapidly quenched Ti-48.8at.%Al-2.2at.%V materials.

The conventionally cast ingots and the top surface of the thickest rapidly solidified materials of this TiAl-V alloy, that have experienced relatively low cooling rates, showed the general features of TiAl alloys where solidification starts with the α phase (5-8). γ was formed from the Al-rich segregated melt in the interdendritic areas while the primary hexagonal dendrites underwent the $\alpha \rightarrow \alpha_2 + \gamma$ solid state transformation resulting in a lath structure made of γ twins with $\alpha_2$ at the interface of some twins.

As long as sufficient melt undercooling was achieved, $\gamma$ was however selected as the first phase to form from the melt. The $\gamma$ solidified dendrites were richer in Al than the interdendritic areas. Thus, with increasing cooling rate the selection of the $\gamma$ metastable phase instead of the $\alpha$ equilibrium phase led to Ti and Al reverse segregation through the ribbon thickness in ribbons thicker than about 200 $\mu$m.

The Al lean areas next to the primary $\gamma$ phase contained 2 types of $\gamma$ lath structures. They are suggested to form from the segregated parent $\alpha$ phase by two different mechanisms. The first structure contained a high density of parallel $\gamma$ laths oriented at 90° to one another around <100> like the one described in (2). This structure was free of any $\alpha_2$ phase. It is suggested that it forms to form via a massive $\alpha \rightarrow \gamma$ transformation. Indeed, a massive transformation has been observed recently in a Ti-48at%Al alloy quenched from the $\alpha$ domain (11). The second structure consisted of {111} twin related $\gamma$ laths with very thin layers of $\alpha_2$ present at some twins boundaries. This structure is associated to the growth of $\gamma$ laths from either the $\alpha$ or $\alpha_2$ phases during the $\alpha \rightarrow \alpha_2 + \gamma$ transformation (9, 10). Observations of other ribbons have shown that the structure of the Al lean interdendritic areas could also be predominantly $\alpha_2$. This is attributed to an incomplete $\alpha \rightarrow \alpha_2 + \gamma$ transformation where $\gamma$ was not allowed to grow from $\alpha_2$ because of a high enough cooling rate (10). The choice of one mechanism instead of the other is likely to be dictated by local differences in cooling rate and chemical composition. For a given chemical composition, the $\alpha$ segregate would transform to $\alpha_2$-free $L1_0$ $\gamma$ laths when the solid state transformation occurs at temperatures lower than $T_0\alpha/\gamma$ which is the thermodynamical condition for massive transformation (12), or transform to $\alpha_2$ when the transformation starts over $T_0\alpha/\gamma$ but with a high enough cooling rate to suppress the complete $\alpha \rightarrow \alpha_2 + \gamma$ process.

At the wheel side of the 20$\mu$m thick ribbons secondary phases were avoided through suppression of solute segregation and $\gamma$ was the only phase present. For the very large melt undercooling involved at the wheel side of our 20$\mu$m thick ribbons, disordered $\gamma$ was formed directly from the melt (2). Although the formation of disordered $\gamma$ has been suggested in Al rich binary TiAl where $\gamma$ is the equilibrium phase to form from the melt (3, 8), direct observation of disordered $\gamma$ has not been reported previously even in rapidly solidified TiAl alloys. This difference between previous studies and this work could be associated with higher cooling rates experienced at the wheel side of our 20 $\mu$m ribbons and the small amount of vanadium in our alloy that could influence the ordering process and the stability of the $\gamma$ phase . Contrary to the "grown in" APBs - associated with the $\alpha \rightarrow \gamma$ tranformation - shown and discussed by Jones and Kaufman (10), the ordered domains - and some possible associated APBs - reported in our TiAl-V alloy resulted from the sequential ordering process of the disordered f.c.c. $\gamma$ phase (2, 4).

## V. Acknowledgement

We would like to thank Prof. J.E. Castle for the provision of research facilities and the Procurement Executive of the Ministery of Defence, U.K., for supporting this work. The authors wish also like to thank Prof. A.P. Miodownik for fruitful discussions.

## VI. References

(1) HUANG S.C. and HALL E.L., *Acta Metall. Mater.*, **39**, (1991), p. 1053.
(2) SHAO G., GROSDIDIER T. and TSAKIROPOULOS P., this conference : "EUROMAT 93".
(3) HALL E.L. and HUANG S.C., *Acta Metall. Mater.*, **38**, (1990), p. 539.
(4) SHAO G., GROSDIDIER T. and TSAKIROPOULOS P., submitted to *Scripta Metal. Mater.*
(5) McCULLOUGH C., VALENCIA J.J., MATEOS H., LEVI C.G. and MEHRABIAN R., *Scripta Metall.*, **22**, (1988), p. 1131.
(6) McCULLOUGH C., VALENCIA J.J., LEVI C.G. and MEHRABIAN R., *Acta Metall.*, **37**, (1989), p. 1321.
(7) VALENCIA J.J., McCULLOUGH C., MATEOS H., LEVI C.G. and MEHRABIAN R., *Acta Metall.*, **37**,

(1989), p. 2517.
(8) ANDERSON C.D., HOFMEISTER W.H., and BAYUSICK R.J., *Met. Trans.*, **23A**, (1992), p. 2699.
(9) KIM Y.W., *Acta Metall. Mater.*, 40, (1992), p. 1121.
(10) JONES S.A. and KAUFMAN M.J., *Acta Metall. Mater.*, 41 , (1993), p. 387.
(11) PING W., VISWANATHAN G.B., and VASUDEVAN V.K., *Met. Trans.*, **23A**, (1992), p. 690
(12) PEREPEZKO J.H., *Met. Trans.*, **15A**, (1984), p. 437.

Table 1 : Chemical composition measurements

| Locations | Structure | Composition at% | | | Methods |
|---|---|---|---|---|---|
| | | Al | Ti | V | |
| Conventionally cast ingot | Hex. dendrite | 49.0 | 48.7 | 2.4 | EPMA |
| | Interdendr. γ | 52.2 | 46.0 | 1.9 | |
| Surface of 400μm flakes | Hex. dendrite | 48.6 | 49.0 | 2.5 | |
| | Interdendr. γ | 49.7 | 48.3 | 2.0 | |
| Mid-section of 150μm ribbons | γ dendrites | 48.4 | 49.4 | 2.2 | AN10000 |
| | Interdendr. γ | 46.2 | 51.7 | 2.1 | |

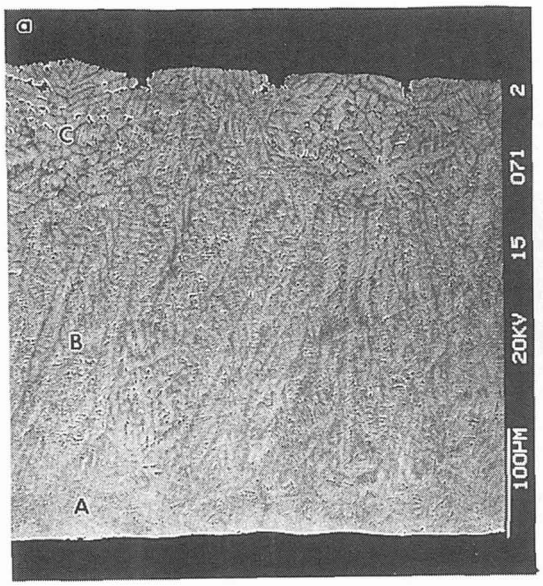


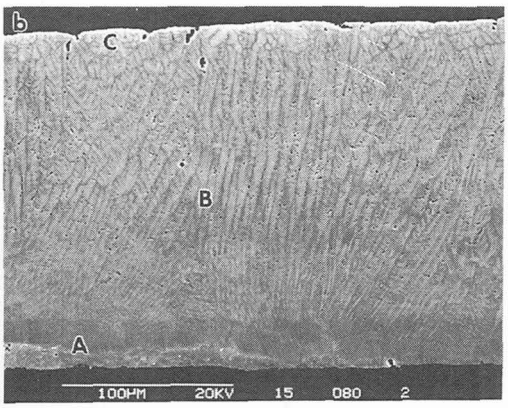


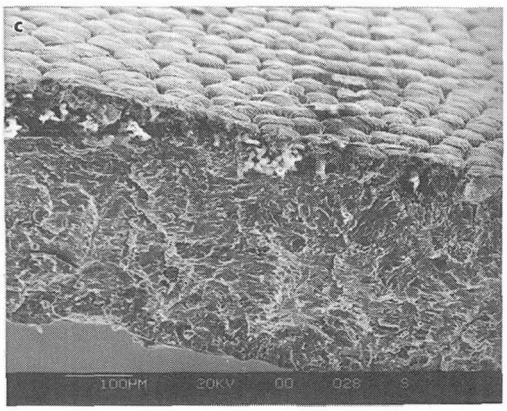


Figure 1 : (a, b) : SEM micrographs of flake transverse sections showing the three zone solidification morphology through the thickness. (c) : SEM micrograph of a fractured surface of a thick flake showing the top surface location of the hexagonal dendritic structure.

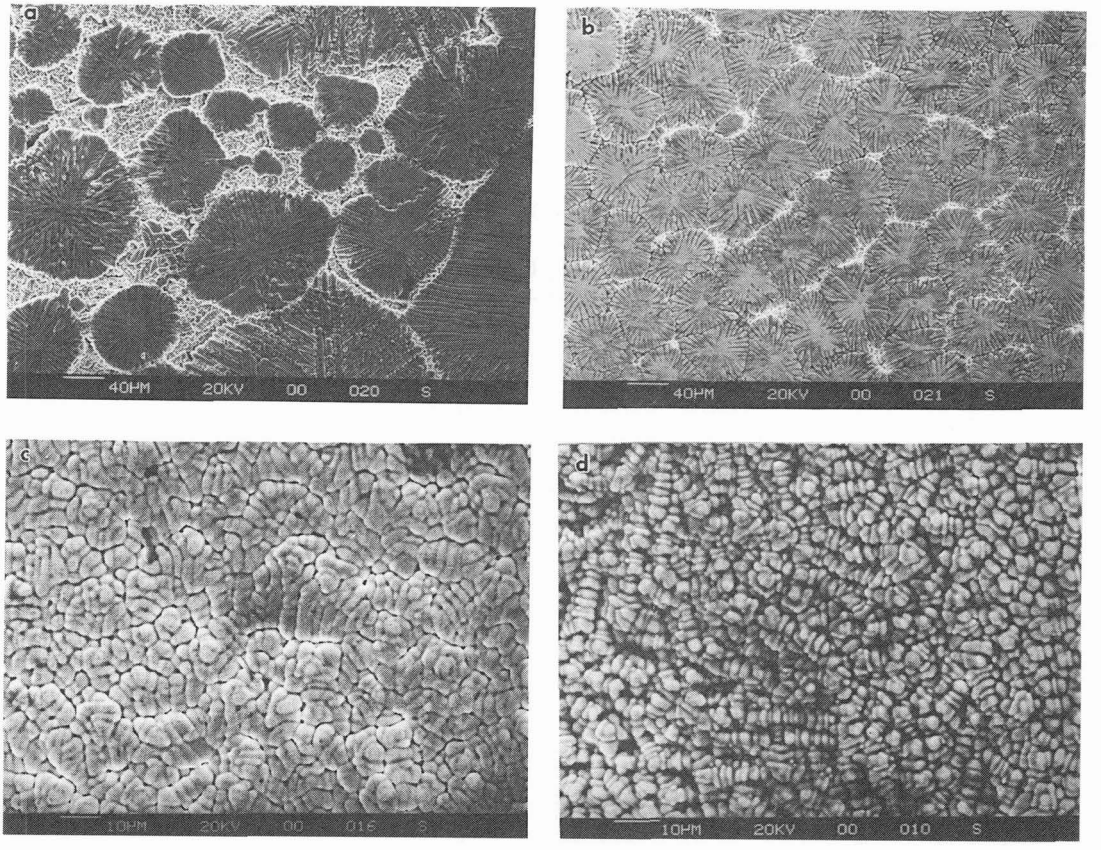


Figure 2 : SEM micrographs showing the different features observed on the top surface of the cast materials of different thicknesses. (a) : 400 µm. (b) : 300 µm. (c) : 100 µm. (a) : 50 µm .

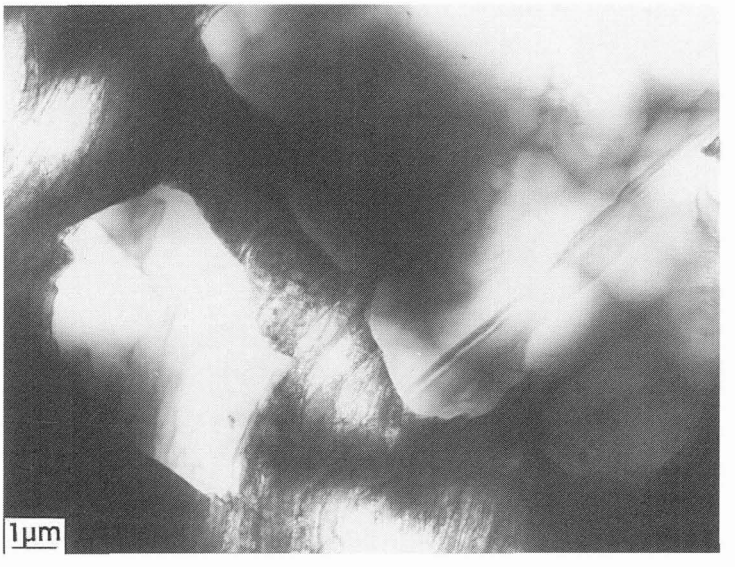


Figure 3 : TEM micrograph showing fine scale features of the microstructure present at the middle section of a 150µm thick material.